J Biol Inorg Chem (2014) 19:59–74
DOI 10.1007/s00775-013-1061-x

ORIGINAL PAPER

Antiproliferative and apoptosis-inducing activity of an oxidovanadium(IV) complex with the flavonoid silibinin against osteosarcoma cells

I. E. Leon · V. Porro · A. L. Di Virgilio · L. G. Naso · P. A. M. Williams · M. Bollati-Fogolín · S. B. Etcheverry

Received: 7 June 2013 / Accepted: 29 October 2013 / Published online: 14 November 2013

Abstract Flavonoids are a large family of polyphenolic compounds synthesized by plants. They display interesting biological effects mainly related to their antioxidant properties. On the other hand, vanadium compounds also exhibit different biological and pharmacological effects in cell culture and in animal models. Since coordination of ligands to metals can improve or change the pharmacological properties, we report herein, for the first time, a detailed study of the mechanisms of action of an oxidovanadium(IV) complex with the flavonoid silibinin, $Na_2[VO(silibinin)_2]\cdot 6H_2O$ (VOsil), in a model of the human osteosarcoma derived cell line MG-63. The complex inhibited the viability of osteosarcoma cells in a dose-dependent manner with a greater potency than that of silibinin and oxidovanadium(IV) ($p < 0.01$), demonstrating the benefit of complexation. Cytotoxicity and genotoxicity studies also showed a concentration effect for VOsil. The increase in the levels of reactive oxygen species and the decrease of the ratio of the amount of reduced glutathione to the amount of oxidized glutathione were involved in the deleterious effects of the complex. Besides, the complex caused cell cycle arrest and activated caspase 3, triggering apoptosis as determined by flow cytometry. As a whole, these results show the main mechanisms of the deleterious effects of VOsil in the osteosarcoma cell line, demonstrating that this complex is a promising compound for cancer treatments.

Keywords Anticancer drug · MG-63 human osteosarcoma cells · Mechanisms of action · Flavonoids · Vanadium

Electronic supplementary material The online version of this article (doi:10.1007/s00775-013-1061-x) contains supplementary material, which is available to authorized users.

I. E. Leon · A. L. Di Virgilio · S. B. Etcheverry
Catedra de Bioquímica Patológica,
Facultad Ciencias Exactas, Universidad Nacional de La Plata,
47 y 115, 1900 La Plata, Argentina

I. E. Leon · A. L. Di Virgilio · L. G. Naso ·
P. A. M. Williams · S. B. Etcheverry (✉)
Centro de Química Inorgánica (CEQUINOR)
Facultad de Ciencias Exactas,
Universidad Nacional de La Plata,
47 y 115, 1900 La Plata, Argentina
e-mail: etcheverry@biol.unlp.edu.ar

V. Porro · M. Bollati-Fogolín
Unidad de Biología Celular,
Institut Pasteur de Montevideo,
Mataojo 2020, 11400 Montevideo, Uruguay

Introduction

Flavonoids are a large family of compounds synthesized by plants that have a common chemical structure [1]. The family includes monomeric flavanols, flavanones, anthocyanidins, and flavones. The interest in the bioactivity of the flavonoids is due, at least in part, to the potential health benefits of these polyphenolic major dietary constituents. It has been shown that flavonoids possess both antioxidative and cytoprotective properties [2].

The biochemical activities of flavonoids depend on their chemical structure. The general pattern that describes their structural arrangements consists of two benzene rings joined by a linear carbon chain of three carbons: C2, C3, C4, represented as the C6–C3–C6 system. The phenolic –OH substituents and the electronic resonance between the A ring and the B ring are the main basis for their antioxidant and biological activities. Besides, the –OH groups

located on the B ring are the most significant factors that influence their scavenging properties towards reactive oxygen species (ROS) [3].

Nevertheless, the mechanism of cell growth regulation is very complex, and therefore the role of ROS in this process depends on the type and concentration of these species. For instance, some antioxidants display a pro-oxidant effect depending on the concentration and environment in which they act [4].

Silibinin, or silybin [3,5,7-trihydroxy-2-[3-(*S*)-(4-hydroxy-3-methoxyphenyl)-2-(*S*)-(hydroxymethyl)-2,3-dihydro-1,4-benzodioxin-6-yl]chroman-4-one] (Fig. 1), a flavonolignan isolated from milk thistle seeds, is the major active constituent of silymarin and one of the popular dietary supplements that has been extensively studied for its antioxidant, hepatoprotective, and anticancer properties [5–7].

Silibinin has also demonstrated potent antiproliferative effects against various malignant cell lines [3], such as human pancreatic carcinoma [8], human bladder carcinoma [7], human prostate adenocarcinoma [9–12], human breast and cervical carcinoma [10], and human colon cancer [13–15] cells. Besides, a comparison of the cancer chemopreventive and anticarcinogenic effects of silymarin and silibinin concluded that the effects of silymarin are due to its major component silibinin [13]. On the other hand, we have previously reported that in the UMR106 rat osteosarcoma cell line silibinin caused a decrease of cell proliferation of approximately 40 % at 100 μM, whereas the decrease of cell proliferation in nontransformed MC3T3-E1 osteoblasts was less than 10 % at the same concentration [16].

Another very broad field of interest is the modulation of flavonoid effects by complex formation to yield flavonoid–metal complexes. In fact, the biological effects of these complexes are more effective than those of free flavonoids, meaning that the physiological and antitumoral properties of flavonoids are enhanced on complexation with metal ions [17, 18]. Nevertheless, coordination complexes of transition metals and silibinin are scarcely reported in the literature, and so far their biological properties have not examined.

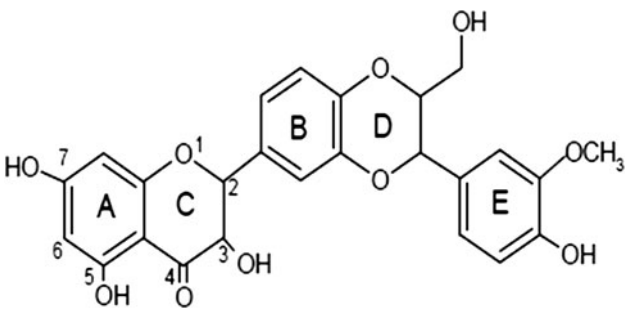

Fig. 1 Chemical structure of silibinin, 3,5,7-trihydroxy-2-[3-(*S*)-(4-hydroxy-3-methoxyphenyl)-2-(*S*)-(hydroxymethyl)-2,3-dihydro-1,4-benzodioxin-6-yl]chroman-4-one

On the other hand, vanadium is an ultratrace element present in higher plants and animals [19, 20]. In vertebrates, after absorption and tissue distribution, great amounts of vanadium are detected in liver, kidney, and especially bones [19].

The biological actions of vanadium convert its compounds into possible therapeutic agents to be used in the treatments of a number of diseases. In particular, vanadate(V) and oxidovanadium(IV) derivatives show insulin-mimetic/antidiabetic activity, growth factor and osteogenic actions [21–23], antitumoral properties [24, 25], cardioprotective actions [26, 27], and neurologic effects [28].

The antitumoral effects of vanadium compounds have been widely investigated on various types of malignant cell lines. Several vanadium compounds produce different effects on cell viability: in some cases they stimulate mitogenesis, but in other cases they inhibit the cell cycle and can also inhibit cell proliferation even at low doses [29, 30]. For this reason, some vanadium compounds may have antitumoral actions [25, 31].

Several mechanisms have been described to explain the inhibition of the cell cycle or the induction of tumor cell death by vanadium derivatives. In particular, the generation of ROS may cause a series of cellular effects such as DNA cleavage, protein tyrosine phosphatase inhibition, and oxidative damage of different cellular components and organelles and finally trigger apoptosis and cell cycle arrest [18, 25, 31].

As part of a project related to the investigation of vanadium compounds with potential pharmacological applications, this study deals with the effects of an oxidovanadium(IV) complex with the flavonoid silibinin, $Na_2[VO(silibinin)_2]\cdot 6H_2O$ (VOsil), on a human osteosarcoma cell line (MG-63). We have investigated and we report herein, for the first time, the action of VOsil on the viability of MG-63 osteosarcoma cells. This tumor cell line derived from a human source is a good model to study the antitumoral actions, cytotoxicity and genotoxicity, and the putative mechanisms involved in the antiproliferative effects of new compounds [32]. In particular, we focus our investigation on the role of oxidative stress and its effects on cytotoxicity, mainly toward lysosomal and mitochondrial metabolism, as well as on cell cycle arrest and apoptosis. Finally, we have investigated the interactions of this compound with cellular DNA.

Materials and methods

Tissue culture materials were purchased from Corning (Princeton, NJ, USA), Dulbecco's modified Eagle's medium (DMEM) and TrypLE™ were purchased from Gibco (Gaithersburg, MD, USA), and fetal bovine serum (FBS) was

purchased from Internegocios (Argentina). Dihydrorhodamine 123 (DHR-123) was purchased from Molecular Probes (Eugene, OR, USA). Annexin V, fluorescein isothiocyanate (FITC), and propidium iodide (PI) were from Invitrogen (Buenos Aires, Argentina). The caspase 3 assay was achieved by means of a commercial kit (Pharmingen^{TM} caspase 3 assay kit, BD). Cytochalasin B from *Dreschslera dematioidea* was purchased from Sigma (St. Louis, MO, USA). Bleomycin (Blocamycin) was kindly provided by Gador (Buenos Aires, Argentina). Syber Green and low melting point agarose were purchased from Invitrogen (Buenos Aires, Argentina). All other chemical were from Sigma (St. Louis, MO, USA).

The MG-63 cell line was purchased from ATCC (CRL1427^{TM}),

Synthesis of VOsil

VOsil was synthesized and identified as in a previous report [16].

Preparations of VOsil solutions

Fresh stock solutions of VOsil and the free form of the ligand were prepared in dimethyl sulfoxide (DMSO) at 20 mM and were diluted according to the concentrations indicated in the legends of the figures. Precautions should be taken with the maximum concentration of DMSO in the well plate. We used 0.5 % as the maximum DMSO concentration in order to avoid toxic effects of this solvent on the osteoblasts.

Cell line and growth conditions

MG-63 human osteosarcoma cells (CRL1427^{TM}) were grown in DMEM containing 10 % FBS, 100 U/mL penicillin, and 100 μg/mL streptomycin at 37° C in a 5 % CO_2 atmosphere. Cells were seeded in a 75-cm^2 flask, and when 70–80 % of confluence was reached, cells were subcultured using 1 mL of TrypLE^{TM} per 25-cm^2 flask. For experiments, cells were grown in multiwell plates. When cells reached the desired confluence, the monolayers were washed with DMEM and were incubated under different conditions according to the experiments.

Peripheral blood mononuclear cells (PBMCs) from healthy and normal donors were isolated from heparinized blood samples through centrifugation on a Ficoll density gradient [33].

Cell viability: crystal violet assay

A mitogenic bioassay was conducted as described by Okajima et al. [34] with some modifications. Briefly, cells were grown in 48-well plates. For experiments, 3×10^4 cells per milliliter were grown for 24 h at 37 °C. Then, the monolayers were incubated for 24 h with different concentrations (2.5–100 μM) of the free form of the ligand or VOsil for the viability assay.

After this treatment, the monolayers were washed with phosphate-buffered saline (PBS) and fixed with 5 % glutaraldehyde/PBS at room temperature for 10 min. Afterward, cells were stained with 0.5 % crystal violet/25 % methanol for 10 min. Then, the dye solution was discarded and the plate was washed with water and dried. The dye taken up by the cells was extracted using 0.5 mL of 0.1 M glycine/HCl buffer, pH 3.0/30 % methanol per well and was transferred to test tubes. After a convenient sample dilution, the absorbance was read at 540 nm. It was previously shown that under these conditions the colorimetric bioassay strongly correlated with cell proliferation measured by cell counting in a Neubauer chamber [22].

Neutral red assay

The neutral red (NR) accumulation assay was performed according to Borenfreund and Puerner [35]. Cells were seeded in 96-well culture plates at a ratio of 2.5×10^4 cells per well. Cells were treated with different VOsil concentrations for 24 h at 37 °C in 5 % CO_2 in air.

After treatment, the medium was replaced by one containing 100 μg/mL NR dye, and the cells were incubated for 3 h. Then, the NR medium was discarded, the cells were rinsed twice with prewarmed (37 °C) PBS to remove the nonincorporated dye, and 100 μL of 50 % ethanol/1 % acetic acid solution was added to each well to fix the cells, releasing the NR into solution. The plates were shaken for 10 min, and the absorbance of the solution was measured with a microplate reader (model 7530, Cambridge Technology, USA) at 540 nm. The optical density was plotted as the percentage of the optical density of the control.

3-(4,5-Dimethylthiazol-2-yl)-2,5-diphenyltetrazolium bromide assay

The 3-(4,5-dimethylthiazol-2-yl)-2,5-diphenyltetrazolium bromide (MTT) assay was performed according to Mosmann [36]. Briefly, cells were seeded in a 96-well dish, allowed to attach for 24 h, and treated with different concentrations of VOsil at 37 °C for 24 h. Afterward, the medium was changed and the cells were incubated with 0.5 mg/mL MTT under normal culture conditions for 3 h. Cell viability was marked by the conversion of the tetrazolium salt MTT to a colored formazan by mitochondrial dehydrogenases. Color development was measured spectrophotometrically with a microplate reader (model 7530, Cambridge Technology, USA) at 570 nm after cell lysis in

DMSO (100 μL per well). Cell viability was plotted as the percentage of the control value.

Cytokinesis-block micronucleus assay

The cytokinesis-block micronucleus assay was set up with cultures in the logarithmic growth phase. Cells were seeded onto precleaned coverslips placed in 35-mm Petri dishes at a density of 3×10^4 cells per dish and were incubated at 37 °C for 24 h. Then, the cells were treated with different concentrations of VOsil with cytochalasin B (4.5 μg/mL) for 24 h. Then, the cells were rinsed and subjected to hypotonic treatment with 0.075 % KCl at 37 °C for 5 min, fixed with pure methanol at −20 °C for 10 min, and stained with 5 % Giemsa solution. After the staining, the coverslips were air-dried and placed onto precleaned slides using Depex mounting medium. For micronucleus assay, 1,000 binucleated cells were scored at ×400 magnification per experimental point from each experiment. The examination criteria used were reported by Fenech [37]. Briefly, the criteria used for identifying micronuclei were as follows: diameter smaller than one third of that of the main nuclei, nonrefractibility, the same staining intensity as or lighter staining intensity than that of the main nuclei, no connection or link with the main nuclei, no overlapping with the main nuclei, and boundary of the micronuclei distinguishable from the boundary of the main nuclei [38].

Single-cell gel electrophoresis assay

For detection of DNA strand breaks, the single-cell gel electrophoresis ("comet") assay was used in the alkaline version, based on the method of Singh et al. [39] with minor modifications. Under alkaline conditions, DNA loops containing breaks lose supercoiling, unwind, and are released from the nuclei and form a "comet tail" by gel electrophoresis. For this experiment, 2×10^4 cells were seeded in a 12-well plate; 24 h later the cells were incubated with various concentrations of VOsil. After 24 h of treatment, cells were suspended in 0.5 % low melting point agarose and immediately poured onto glass microscope slides. Slides were immersed in ice-cold lysis solution in darkness for 1 h (4 °C) in order to lyse the cells, remove cellular proteins, and allow DNA unfolding. Immediately afterward, the slides were put in a horizontal electrophoresis tank containing 1 mM Na_2EDTA and 0.3 M NaOH (pH 12.7), and then electrophoresis was performed for 30 min at 25 V (4 °C). Afterward, the slides were neutralized and stained with Syber Green. Analysis of the slides was performed with an Olympus BX50 fluorescence microscope. Images of cells were acquired with Leica IM50 Image Manager (Imagic Bildverarbeitung). A total of 50 randomly captured cells per experimental point of each experiment were used to determine the tail moment (product of the tail length and the tail DNA percentage) using a free comet scoring program (Comet Score version 1.5). Two parallel slides were analyzed for each experimental point. Independent experiments were repeated twice. A 20-min pulse of 10 μg/mL bleomycin just before the cells were harvested was used as a positive control..

Determination of ROS production

Oxidative stress in osteoblasts was evaluated by measurement of intracellular production of ROS after incubation of the cell monolayers with different concentrations of VOsil for 4 h at 37 °C. ROS generation was determined by oxidation of DHR-123 to rhodamine by spectrofluorimetry as we have previously described [40].

Fluorometric determination of cellular reduced glutathione and oxidized glutathione levels

Reduced glutathione (GSH) and oxidized glutathione (GSSG) levels were determined in osteoblasts in culture as follows. Confluent osteoblast monolayers from 24-well dishes were incubated with different concentrations of VOsil at 37 °C for 24 h. Then, the monolayers were washed with PBS and harvested by incubating them with 250 μL of 0.1 % Triton for 30 min. For GSH determination, 100-μL aliquots were mixed with 1.8 mL of ice-cold phosphate buffer (0.1 M Na_2HPO_4/0.005 M EDTA, pH 8) and 100 μL *o*-phthaldialdehyde (0.1 % in methanol) as described by Hissin and Hilf [41]. For the determination of GSSG, 100-μL aliquots were mixed with 1.8 mL of 0.1 M NaOH and *o*-phthaldialdehyde as before. Previously, to avoid GSH oxidation, the cellular extracts for GSSG determination were incubated with 0.04 M *N*-ethylmaleimide. Fluorescence at an emission wavelength of 420 nm was determined after excitation at 350 nm. Standard curves with different concentrations of GSH were processed in parallel. The protein content in each cellular extract was quantified using the Bradford assay [42]. The ratio of GSH to GSSG, which is a better marker for the cellular redox status, was calculated as the percentage of the basal level for all experimental conditions.

Measurement of externalization of phosphatidylserine by annexin V–FITC/PI staining

Cells in early and late stages of apoptosis were detected with annexin V–FITC and PI staining. Cells were treated with 25 and 100 μM VOsil and were incubated for 6 and 24 h prior to analysis. For the staining, cells were washed

with PBS and adjusted to a concentration of 1×10^6 cells per milliliter in 1× binding buffer. To 100 µL of cell suspension, 2.5 µL of annexin V–FITC was added and the mixture was incubated for 15 min at room temperature. Finally, 2 µL PI (250 µg/mL) was added prior to analysis. Cells were analyzed using a CyAn™ ADP flow cytometer (Beckman Coulter, USA) and Summit version 4.3. For each analysis, 10,000 counts, gated on a forward scatter versus side scatter dot plot, were recorded. Four subpopulations were defined in the dot plot: the undamaged vital (annexin V negative/PI negative), the vital mechanically damaged (annexin V negative/PI positive), the apoptotic (annexin V positive/PI negative), and the secondary necrotic (annexin V positive/PI positive)subpopulations.

Caspase 3 assay

The determination of caspase 3, one of the main effector caspases, was conducted with a commercial kit (Pharmingen™ caspase 3 assay kit, BD) following the recommendation of the manufacturer. Briefly, cells were grown in 24-well plates for 24 h (3×10^5 cells per well). Then, the monolayers were incubated with different concentrations of VOsil (25 and 100 µM) for 6 h. After this treatment, the monolayers were washed with PBS and were harvested with trypsin at 37 °C for 5 min. Afterward, 1× Cytofix/Cytoperm buffer was added and the mixture was incubated in an ice-cold bath for 20 min. Then, the cells were centrifuged at 1,000 rpm for 5 min and were finally collected. Afterward, anticaspase 3 FITC antibody was added and the mixture was incubated for 30 min at room temperature. Then, the cells (10,000 events) were analyzed using a CyAn™ ADP flow cytometer (Beckman Coulter, USA) and Summit version 4.3.

Measurement of cell cycle/DNA content

The DNA content in G_1/G_0, S, and G_2/M phases was analyzed using flow cytometry [43, 44].

Cells were seeded in six-well plates, cultured for 24 h, and then treated with 25 and 100 µM VOsil for 6 and 24 h. The harvested cells were washed with PBS, fixed, and permeabilized with 70 % ice-cold ethanol for more than 2 h. Subsequently, the cells were resuspended in fresh staining buffer (15 mg/mL PI and 15 mg/mL DNase-free RNase prepared in PBS containing 2 mM EDTA) and incubated for 30 min at 37 °C. Cell cycle distribution analysis was performed with a CyAn™ ADP flow cytometer using Summit version 4.3 for data acquisition. For each sample, cellular aggregates were gated out and at least 10,000 cells were counted and plotted on a single-parameter histogram. Experiments were performed following the guidelines described by Hurley et al. [43].

The percentage of cells in the G_1/G_0, S, and G_2/M phases and the sub-G_1 peak was then calculated using FlowJo 7.6 (using the Watson model).

Statistical analysis

At least three independent experiments were performed for each experimental condition in all the biological assays. The results are expressed as the mean ± the standard error of the mean. Statistical differences were analyzed using the analysis of variance method followed by the test of least significant difference (Fisher).

Results

Effect of chemical complexation on cell viability in MG-63 cells

To test the effect of chemical complexation on cell viability, human MG-63 osteosarcoma cells were exposed to the flavonoid silibinin, the oxidovanadium(IV) cation, and VOsil. As can be seen in Fig. 2, the oxidovanadium(IV) cation caused an inhibitory effect only at 100 µM, whereas silibinin and VOsil diminished the cell viability from 25 µM ($p < 0.01$). However, VOsil was the strongest antiproliferative agent in the range from 25 to 75 µM ($p < 0.05$), whereas at 100 µM, the antitumoral actions of VOsil and silibinin did not show significant differences ($p < 0.05$). These results demonstrate the beneficial effect

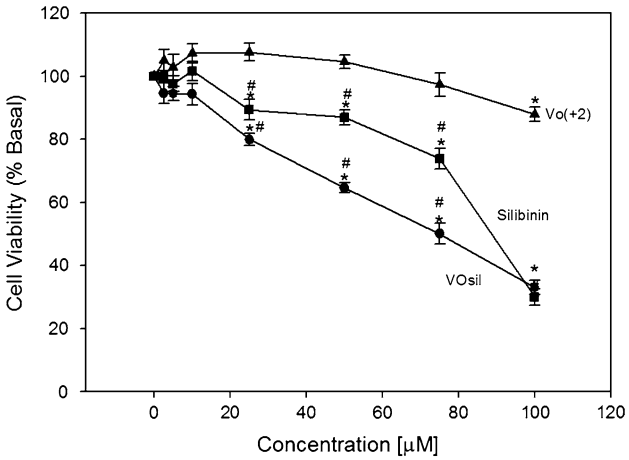

Fig. 2 Effects of $Na_2[VO(silibinin)_2]\cdot 6H_2O$ (*VOsil*) on MG-63 human osteosarcoma cell line proliferation. Cells were incubated in serum-free Dulbecco's modified Eagle's medium (DMEM) alone (control) or with different concentrations of VOsil at 37 °C for 24 h. The results are expressed as the percentage of the basal level and represent the mean ± the standard error of the mean (SEM) ($n = 18$). *Asterisk* significant difference in comparison with the basal level ($p < 0.01$)

of complexation on the antitumoral action. The half-maximal inhibitory concentrations in MG-63 cells are 74 μM for VOsil, 89 μM for silibinin, and more than 100 μM for oxidovanadium(IV). According to these results, the following potency order can be established for the antitumoral action: VOsil > silibinin > VO^{2+}.

To determine the antitumoral effectiveness of VOsil, we compared its effects with those of the reference metallodrug (cisplatin) in MG-63 cells. In the lower concentration range (2.5–10 μM) cisplatin and VOsil did not have any effect on cell viability. At 25 μM, the effects of cisplatin and VOsil were similar since both of them produced a decrease in cell viability of approximately 15 %. At 50 μM, VOsil was less deleterious than cisplatin (60 % survival vs 23 % survival), whereas at 100 μM the differences were 33% versus 21 % surviving cells, respectively.

Effect of VOsil on the viability of PBMCs

To understand the real potential of VOsil and to address its selectivity for cancer cells, we investigated its effect on the viability of PBMCs. Figure 3 shows the effect of VOsil on the viability of PBMCs. As can be seen, at 25 and 50 μM, VOsil did not alter the cellular viability of PBMCs, and only at 100 μM could a slight decrease (approximately 15 %) in cell survival be detected ($p < 0.01$). Considering the deleterious effect of VOsil on the MG-63 tumor cell line and on PBMCs, the promising action of VOsil has been shown.

Cytotoxicity studies

To obtain deeper insight into the antiproliferative effects of VOsil, the cytotoxicity of the complex toward two relevant organelles of the cells—lysosomes and mitochondria—was investigated through the NR uptake and the reduction of MTT assays, respectively.

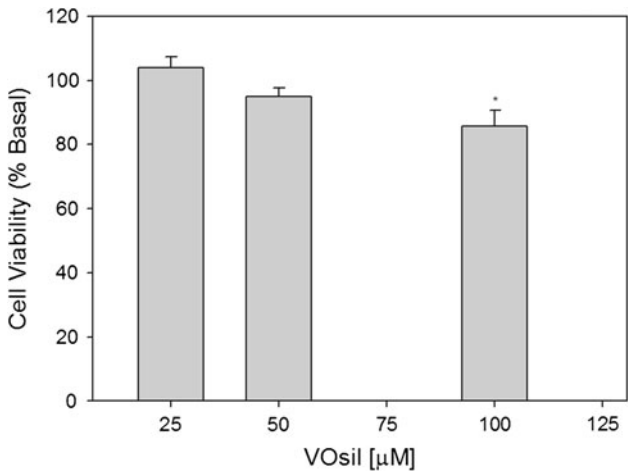

Fig. 3 Effects of VOsil on proliferation of peripheral blood mononuclear cells. Cells were incubated with 25, 50, and 100 μM VOsil at 37 °C for 24 h. The results are expressed as the percentage of the basal level and represent the mean ± SEM ($n = 9$). *Asterisk* significant difference in comparison with the basal level ($p < 0.01$)

The NR technique is used to measure the growth of a population of cultured cells: viable cells take up the NR dye and transport it to the lysosomes. The uptake, transport, and storage of the NR dye require energy, as well as intact cellular and lysosomal structures [35]. The metabolically active lysosomes display the capacity of take up the NR dye. A loss of lysosomal activity, indicated by a decrease in the uptake of NR, was observed when MG-63 cells were exposed to increasing concentrations of VOsil (Fig. 4a). The data presented herein show a cytotoxic effect of VOsil in a concentration-dependent manner from 25 to 100 μM with statistically significant differences versus the control (without complex addition) ($p < 0.01$).

The alteration in the energetic metabolism of the cells was determined by the MTT assay. This technique measures the ability of the mitochondrial succinic dehydrogenases to reduce the methyl tetrazolium salt [36]. Figure 4b shows the effects of VOsil on mitochondrial metabolism of MG-63 osteosarcoma cells. A concentration-related inhibition was observed from 25 to 100 μM with statistically significant differences versus the basal condition ($p < 0.01$). These results are in agreement with the effect of VOsil on lysosomal metabolism.

Effect of serum components on the antitumoral action of VOsil in MG-63 osteosarcoma cells

To test the effects of VOsil under more natural conditions, the antiproliferative action of VOsil in MG-63 cells was tested in the presence of 10 % FBS since VOsil could interact with the serum components and its antitumoral activity could be modified by interactions with the serum components. The results obtained in the presence of 10 % FBS plus different concentrations of VOsil for cell viability (crystal violet bioassay) and for the cytotoxicity of VOsil (MTT assay) can be seen in Fig. 5. No statistical differences from the previous results (serum-free experiments) were determined, indicating that the serum components have no impact on the effects of VOsil on the osteosarcoma cells.

Genotoxicity studies

The genotoxic effects of VOsil were investigated through the increase of the micronucleus frequency and the induction of DNA damage by the comet assay.

Micronuclei are cytoplasmic bodies having a portion of an acentric chromosome or the whole chromosome which was not carried during anaphase, thus resulting in whole chromosomes or parts of them being missing from the main

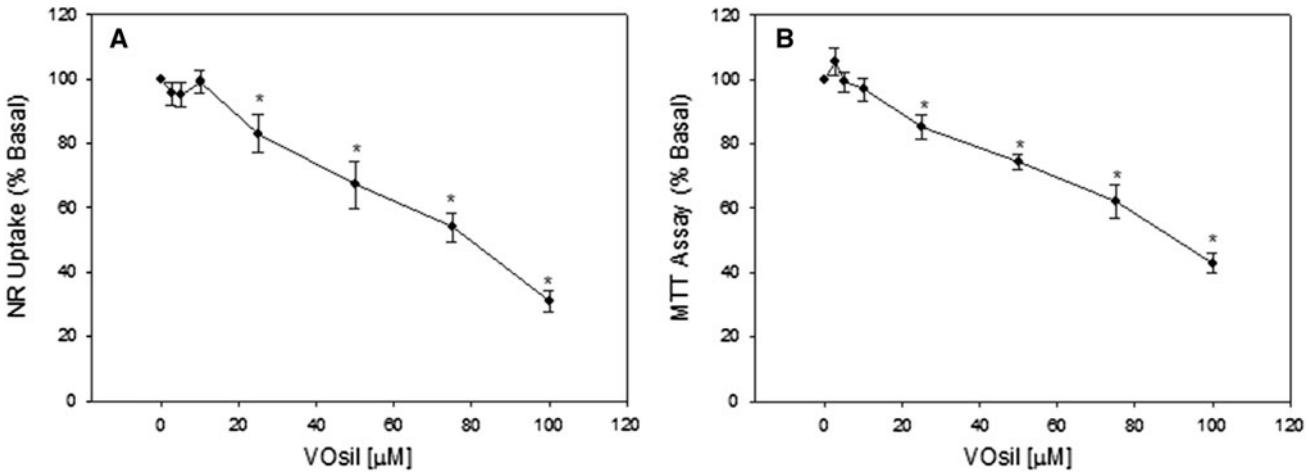

Fig. 4 **a** Neutral red (*NR*) uptake by MG-63 osteosarcoma cells in culture. Tumor cells were incubated with different concentrations of VOsil for 24 h at 37 °C. After incubation, cell viability was determined by the uptake of NR. The dye taken up by the cells was extracted and the absorbance was read at 540 nm. The results are expressed as the percentage of the basal level and represent the mean ± SEM ($n = 18$). *Asterisk* $p < 0.01$. **b** Evaluation of the mitochondrial succinate dehydrogenase activity by the 3-(4,5-dimethylthiazol-2-yl)-2,5-diphenyltetrazolium bromide (*MTT*) assay in MG-63 cells in culture. Osteosarcoma cells were incubated with different doses of VOsil for 24 h at 37 °C. After incubation, cell viability was determined by the MTT assay. The results are expressed as the percentage of the basal level and represent the mean ± SEM ($n = 18$). *Asterisk* $p < 0.01$

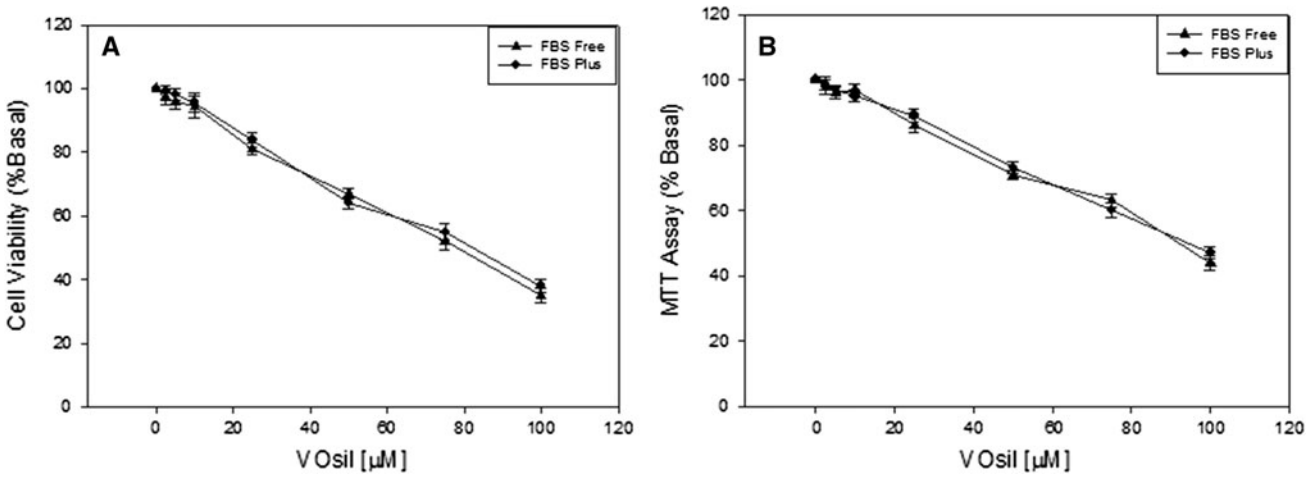

Fig. 5 **a** Effects of VOsil on MG-63 human osteosarcoma cell line proliferation. Cells were incubated in serum-free DMEM (*triangles*) and in the presence of 10 % fetal bovine serum (*FBS*) (*circles*) with different concentrations of VOsil at 37 °C for 24 h. The results are expressed as the percentage of the basal level and represent the mean ± SEM ($n = 18$). **b** Evaluation of the mitochondrial succinate dehydrogenase activity by the MTT assay in MG-63 cells in culture. Osteosarcoma cells were incubated in serum-free DMEM (*triangles*) and in the presence of 10 % FBS (*circles*) with different concentrations of VOsil at 37 °C for 24 h. After incubation, cell viability was determined by the MTT assay. The results are expressed as the percentage of the basal level and represent the mean ± SEM ($n = 18$)

nuclei [45]. The effect of VOsil on the induction of micronuclei in binucleated cells can be observed from Fig. 6a. In MG-63 cells, VOsil induced micronucleus formation with similar values from 2.5 to 10 μM, nearly triple the level of the control group ($p < 0.01$).

The comet assay detects single-strand and double-strand DNA breaks. Additional DNA damage is detected, such as abasic sites (missing either a pyrimidine or a purine nucleotide) and sites where excision repair is detected under alkaline conditions [46]. We evaluated the tail moment parameter, which is defined as the product of the tail length and the amount of DNA amount in the tail. The amount of DNA is determined through the intensity of fluorescence. The distance of DNA migration is used to measure the extent of DNA damage. However, if the amount of DNA damage is relatively high, the tail increases in fluorescent staining intensity but not in length [47]. Thus, for these reasons it is useful to use the tail

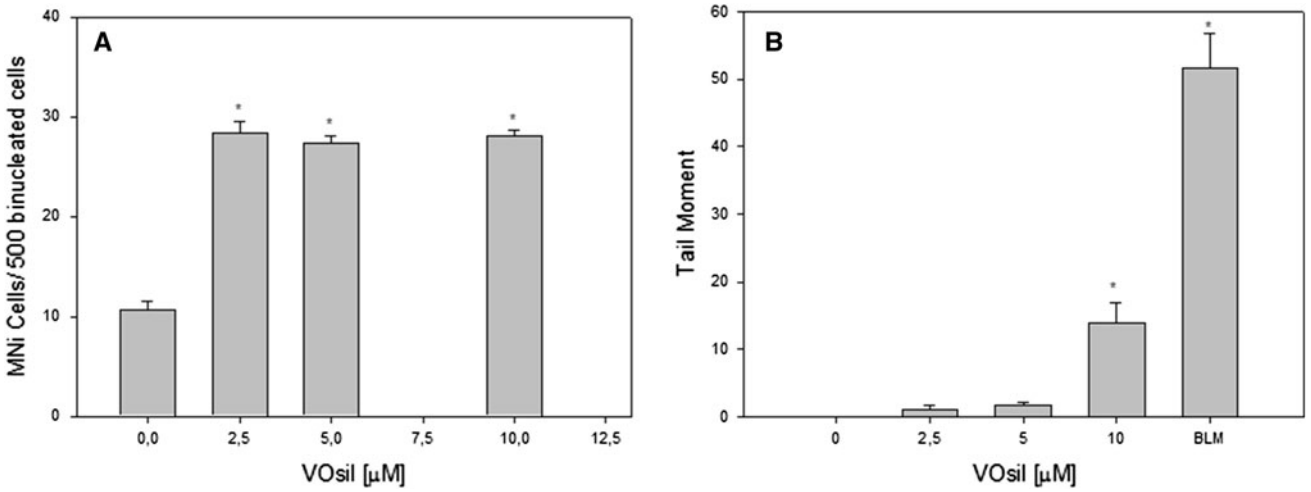

Fig. 6 Genotoxicity of VOsil toward MG-63 tumor cells. **a** Micronucleus assay: induction of micronuclei in MG-63 cells after 24 h exposure to VOsil. *Asterisk* significant difference at $p < 0.001$. **b** Comet assay: single-cell gel electrophoresis. Induction of DNA damage by VOsil in the MG-63 human osteosarcoma cell line. DNA damage was evaluated by the tail moment. After incubation with VOsil for 24 h, cells were lysed and DNA fragments were processed by electrophoresis. After electrophoresis, the nuclei were stained and analyzed. The results are expressed as the mean ± SEM ($n = 150$). *Asterisk* $p < 0.001$. Bleomycin (*BLM*) was used as a positive control. *MNi* micronuclei

moment as a genotoxic end point. As shown in Fig. 6b, VOsil produced a significant genotoxic effect in MG-63 cells from 10 μM ($p < 0.01$). Altogether, these results suggest that VOsil induced single-strand and double-strand DNA breaks in MG-63 cells, leading to a positive result in the comet assay and induction of micronuclei, which is significantly detected at lower concentrations.

Mechanism of action

The putative cell death mechanisms triggered by VOsil were investigated through the determination of the oxidative stress (by means of ROS production), GSH levels, and the GSH/GSSG redox couple. Moreover, an exhaustive study of apoptosis and cell cycle arrest was also performed.

Oxidative stress and GSH/GSSG status

Oxidative stress has been reported as one of the main factors that trigger the deleterious actions of vanadium compounds [25, 40, 48–51].

For a better understanding of the possible mechanism involved in the cytotoxicity of VOsil in MG-63 cells, we evaluated the effect of VOsil on oxidative stress through the oxidation of the probe DHR-123 and the ratio of GSH to GSSG.

DHR-123 is a mitochondria-associated probe that selectively reacts with hydrogen peroxide [40, 52]. Incubation of MG-63 osteosarcoma cells with VOsil caused an increase in the production of ROS, as can be observed in Fig. 7A. At 100 μM, VOsil increased ROS production after 6 h of incubation, whereas at 25 μM no production of ROS over the basal level could be observed ($p < 0.01$). To confirm the role of VOsil in the generation of ROS, a test using scavengers such as a mixture of vitamins C and E was performed under the same experimental conditions. As can be seen in Fig. 7b, at 100 μM the level of ROS decayed in the presence of the scavengers, reaching the control value ($p < 0.01$). This experiment demonstrated that oxidative stress was triggered by VOsil and ROS production could be considered as one of the relevant mechanisms of action of VOsil. To confirm that the increase of ROS levels is relevant to cell viability, experiments with the crystal violet bioassay were conducted in the presence of a mixture of vitamins C and E. Figure 7c displays the effect of the scavengers on cell proliferation. Cell viability was completely recovered when the concentration of VOsil was 75 μM, whereas at 100 μM the deleterious effect of the drug was partially overcome ($p < 0.01$).

To study the deleterious effect of VOsil at a longer time (24 h), we tested the concentration range (25–100 μM) of VOsil. Statistically significant differences could be seen at 50 and 100 μM ($p < 0.01$). At the highest concentration, VOsil caused a 311 % increase of ROS production over the basal level (Fig. 8). Under this experimental condition (24 h), the cell viability could not be recovered by the scavengers in the whole concentration range, suggesting that the levels of ROS and damage were very high.

To obtain broader knowledge of the factors involved in the cellular redox status, the ratio of GSH to GSSG was investigated. GSH is one of the major reducing agents in

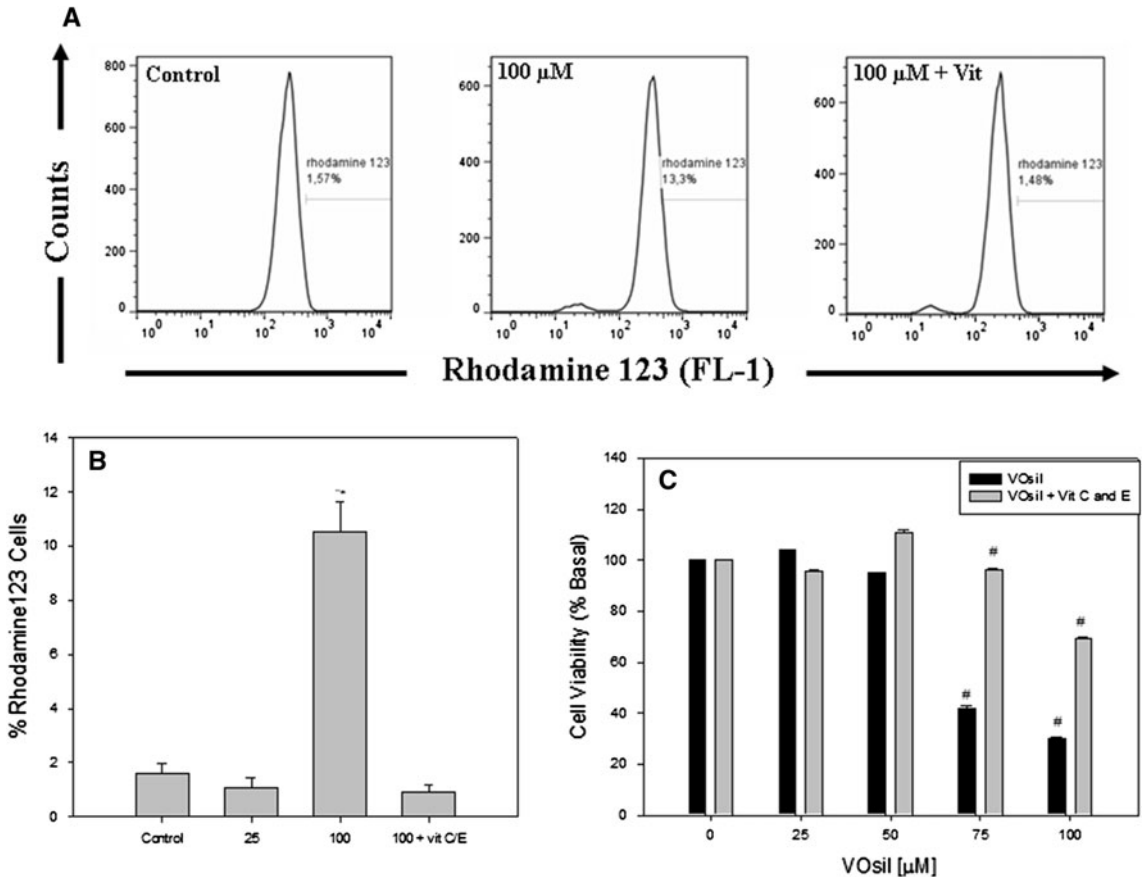

Fig. 7 **a** Short-time induction of reactive oxygen species (ROS) by VOsil in the MG-63 cell line. Cells were incubated with 25 and 100 µM VOsil at 37 °C for 6 h. ROS production in the cells was evaluated through the oxidation of dihydrorhodamine 123 (DHR-123) to rhodamine 123 (flow cytometry). **b** The effect of the induction of ROS by VOsil in the MG-63 cell line. The results represent the mean ± SEM ($n = 9$). The plots are representative of three independent experiments. *Asterisk* significant differences versus the control ($p < 0.01$), *vit C/E* mixture of vitamins C and E. **c** Effect of VOsil on MG-63 cell viability in the presence of a mixture of vitamins C and E (each at 50 µM). Cells were incubated with different concentrations of VOsil and a mixture of the vitamins at 37 °C for 24 h. The results are expressed as the mean ± SEM ($n = 18$). *Number sign* significant differences between treatments ($p < 0.05$)

mammalian cells. This thiol acts by sequestering free radicals and regulating the redox status by means of the GSH/GSSG couple [53]. A sustained increase in ROS levels may cause an accumulation of GSSG inside cells. Because of this, the determination of the ratio of GSH to GSSG is relevant in the investigation of oxidative stress [54].

As can be seen from Fig. 9a, VOsil induced a decrease in the ratio of GSH to GSSG in MG-63 cells in a concentration-dependent manner ($p < 0.01$).

To confirm that the depletion of GSH played a role in the cytotoxic effect of VOsil in MG-63 cells, viability experiments were performed in the presence of VOsil plus 1 mM GSH. The results can be seen in Fig. 9b. At 25 uM VOsil, the surviving cells account for 93 % of the total cells in relation to the control, whereas in the absence of the thiol, this fraction was 79 %, indicating a recovery of 14 % in the presence of GSH. At 100 µM VOsil, the recovery was 11 %.

Overall, it can be assumed that the free radicals decrease the concentration of important cellular compounds and impair the antioxidant system, making cells more vulnerable to oxidative damage.

Apoptosis study

Apoptosis is a physiological process of cell death enhanced in the presence of harmful agents. It produces various modifications in cell structure. Cell death may be triggered by an extrinsic pathway mediated by receptors on the surface of the cells or can be produced by endoplasmic reticulum or mitochondrial stress (intrinsic pathway). As a consequence, a genetic program that leads to cell death is activated. Apoptosis is characterized by some morphological changes in the nucleus and the cytoplasm. Because of this, apoptosis can be assessed by using several characteristic features of programmed cell death. One of the first alterations that can be defined is the externalization of

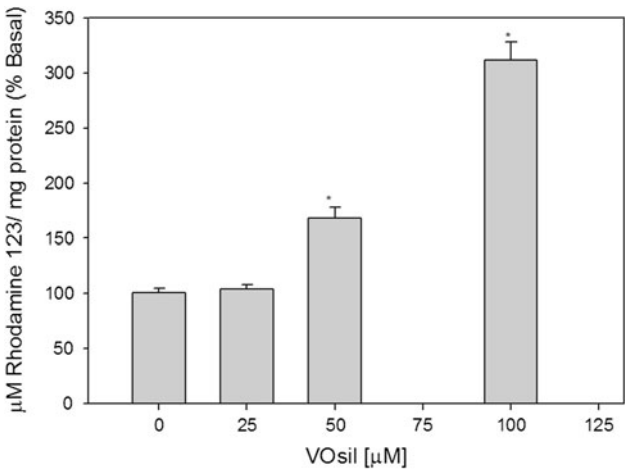

Fig. 8 Induction of ROS by VOsil in the MG-63 cell line at 24 h. Cells were incubated with increasing concentrations of VOsil at 37 °C for 24 h. ROS production in the cells was evaluated through the oxidation of DHR-123 to rhodamine 123 (spectrofluorimetry) and was normalized to micromoles of rhodamine 123 per liter per milligram of protein (percentage of the basal value). The results represent the mean ± SEM ($n = 12$). *Asterisk* significant difference versus the control ($p < 0.01$)

phosphatidylserine at the outer plasma membrane leaflet. Other features of apoptosis are the activation of the caspase pathway and DNA fragmentation.

Effects of VOsil on phosphatidylserine externalization

Independently of the cell type and the nature of the injuring agent, the externalization of phosphatidylserine is always present in the earlier apoptotic events. Annexin V–FITC is a fluorescent probe with high affinity for phosphatidylserine, allowing its determination by fluorescence assays. Figure 10 depicted the flow cytometry results of the apoptotic process in the presence of VOsil (25 and 100 μM).

Moreover, to obtain deeper insight into the apoptosis induced by VOsil, we tested two concentrations of the complex (25 and 100 μM) and two incubation times (6 and 24 h). Table 1 displays the quantification of early and late stages of apoptosis obtained by flow cytometry in MG-63 cells.

Table 1 shows that after 6 h of incubation, the control cultures showed 10 % of early apoptotic cells were annexin V positive and 4 % of late apoptotic cells were annexin V positive/PI positive. These results changed at 24 h, showing an increase in the late apoptotic cellular fraction (16 %) and a decrease in the fraction of early apoptotic cells (4 %). After 6 h of treatment, VOsil resulted in approximately 29 % and 32 % early apoptotic cells (annexin V positive) at 25 and 100 μM, respectively. Nevertheless, only at 100 μM did VOsil produce 28 % of cells of late apoptotic features, with a statistically significant difference with the control and the results obtained with 25 μM VOsil ($p < 0.01$). On the other hand, after 24 h of treatment, VOsil resulted in approximately 37 % early apoptotic cells and 29 % late apoptotic cells at 25 μM, whereas at 100 μM, VOsil produced a striking increase in the fraction of late apoptotic cells (See Fig. 10).

As can be seen, the percentages of apoptotic and apoptotic/necrotic cells increased with the concentration of VOsil and the exposure time. These results are in accordance with the viability assays, confirming that the deleterious action of VOsil is dependent on its concentration in the MG-63 cell line.

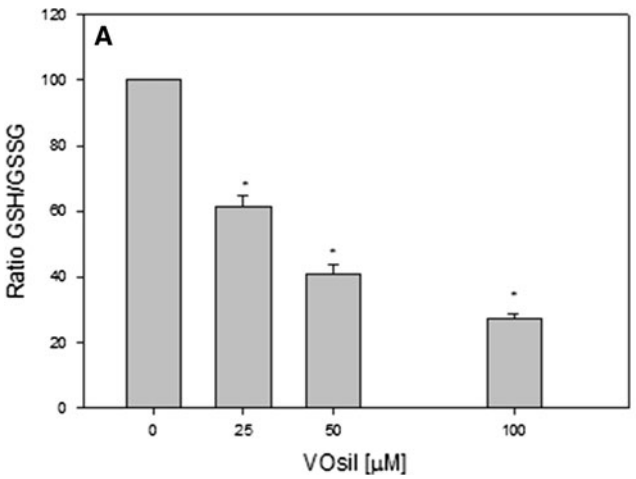

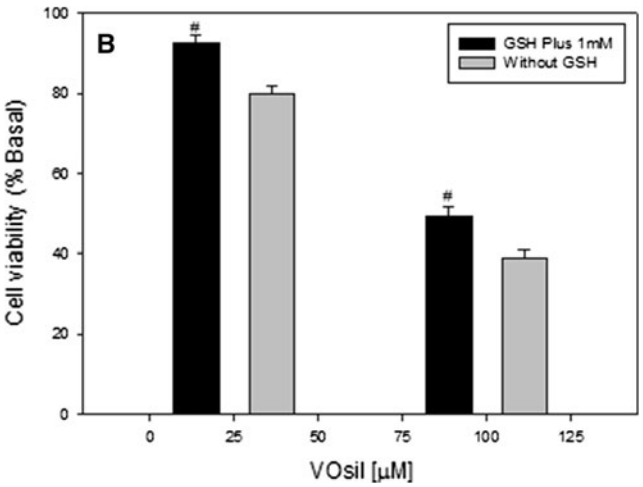

Fig. 9 **a** Ratio of reduced glutathione (*GSH*) to oxidized glutathione (*GSSG*) in MG-63 cells incubated with different concentrations of VOsil. The results are expressed as the mean ± SEM of three independent experiments. *Asterisk* significant differences versus the basal level ($p < 0.01$). **b** Effect of VOsil on MG-63 cell viability in the presence of GSH. Cells were incubated for 2 h with 1 mM GSH and then different concentrations of VOsil were added at 37 °C for 24 h. The results are expressed as the mean ± SEM ($n = 18$). *Number sign* significant differences between treatments ($p < 0.05$)

Table 1 Percentage of apoptotic cells treated with $Na_2[VO(silibinin)_2]\cdot 6H_2O$ (*VOsil*)

VOsil (μM)	Annexin V positive		Annexin V positive/PI positive	
	6 h	24 h	6 h	24 h
0	10	5	4	16*
25	29*	37*	4	29*
100	32*	41*	28*	58*

The results are expressed as the mean ± the standard error of the mean of three independent experiments ($n = 9$)

PI propidium iodide

* Significant differences versus the control ($p < 0.01$)

Caspase 3 activation

Caspases (cysteine-requiring aspartate proteases) are a family of proteases that mediate cell death and are important to the process of apoptosis. Caspase 3 is one of the critical members of this family. It is an effector caspase that cleaves most of the caspase-related substrates involved in apoptosis regulation [55–57]. Caspase 3 plays a central role in mediating nuclear changes, including chromatin condensation and DNA fragmentation as well as cell blebbing [58].

In Figs. 11 and S1, it can be seen that after 6 h of incubation of the cells with VOsil, caspase 3 is activated only at 100 μM ($p < 0.01$), demonstrating that the apoptotic action of VOsil is in agreement with the annexin V assay (28 % late apoptotic cells at 6 h). The activation of caspase 3 is a good marker to confirm the annexin V results for the detection of late apoptosis.

Cell cycle analysis and DNA fragmentation

Cells go through the cell cycle in several well-controlled phases [59]. The entry into each phase of the cell cycle is carefully regulated by different checkpoints. One theme emerging from drug discovery is to develop agents that target the cell cycle checkpoints that are responsible for the control of cell cycle phase progression.

Endonucleases activated during apoptosis target internucleosomal DNA sections and cause extensive DNA fragmentation [60–62]. Apoptotic cells have deficient DNA content, and when stained with a DNA-specific fluorochrome, they can be recognized by flow cytometry as cells with less DNA than G_1 cells, known as the "sub-G_1" peak in the DNA content frequency histograms [43, 44, 63]. Loss of DNA may also occur as a result of the shedding of apoptotic bodies containing fragments of nuclear

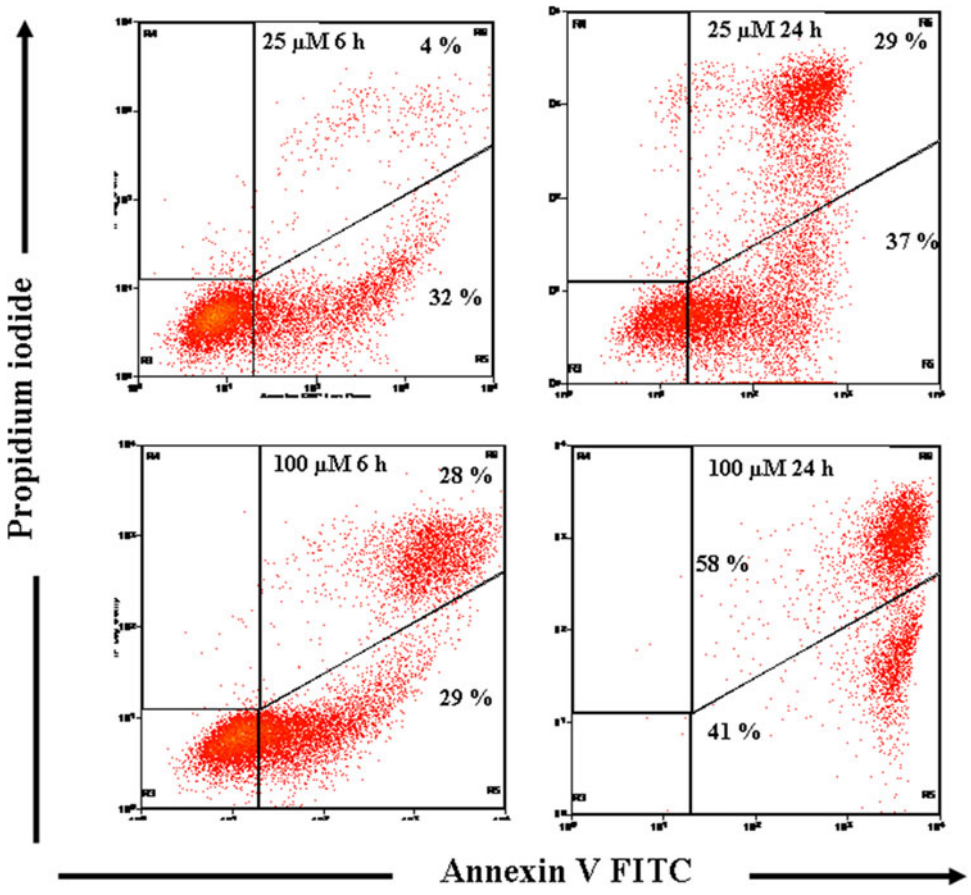

Fig. 10 Effect of VOsil on apoptosis assessed by flow cytometry using annexin V–fluorescein isothiocyanate (*FITC*)/propidium iodide (PI) staining. MG-63 cells were treated with VOsil at 0 μM (control), 25 μM, and 100 μM at 37 °C for 6 and 24 h. The plots are representative of three independent experiments. The *numbers* in the R5 and R6 quadrants indicate the proportions of cells that are annexin V positive/PI negative and annexin V positive /PI positive, respectively

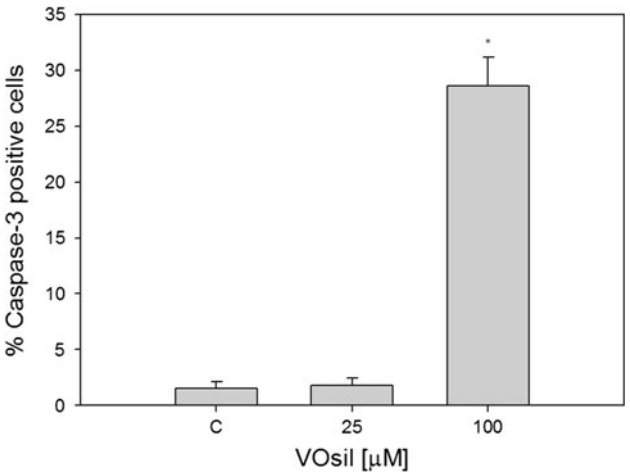

Fig. 11 Effect of VOsil on activity of caspase 3. Activity of caspase 3 was determined with the caspase 3 specific antibody coupled FITC. MG-63 cells were treated with VOsil at 0 μM (control), 25 μM and 100 μM at 37 °C for 6 h and were then harvested and analyzed by flow cytometry. The results are expressed as the mean ± SEM of three independent experiments ($n = 9$) *Asterisk* significant differences versus the control ($p < 0.01$)

chromatin. The degree of DNA degradation depends on the stage of apoptosis, the cell type, and often the nature of the apoptosis-inducing agent.

Cell cycle arrest and the progression of apoptosis as a function of the concentration of VOsil and the incubation time were analyzed by flow cytometry. As shown in Fig. 12, after 6 h of incubation with 25 μM VOsil, the cell cycle distribution was not affected. On the other hand, with 100 μM VOsil, cells were arrested at G_2/M phase ($p < 0.05$). Moreover, after 24 h (Fig. 12), VOsil induced apoptosis (evaluated by the sub-G_1 peak) at both concentrations analyzed, which seems to be associated with cell cycle arrest in G_2/M phase.

The deleterious actions of VOsil are a function of its concentration and the incubation time, with an exacerbation of the effects at higher concentrations and longer times.

Discussion

Recently, there has been increasing interest in the antitumoral effects of vanadium derivatives [24, 25]. It was

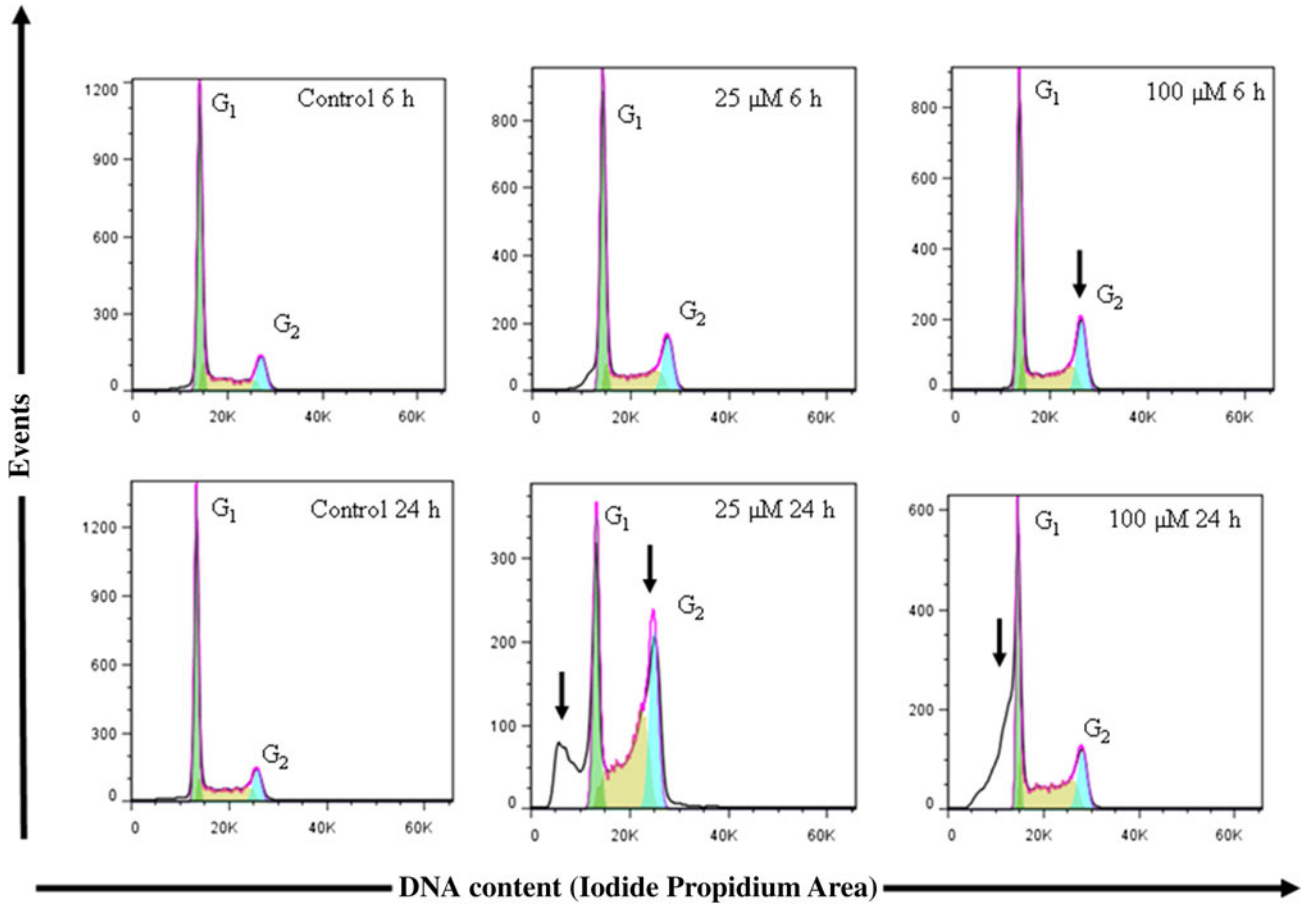

Fig. 12 Effect of VOsil on cell cycle arrest and DNA fragmentation. The plots are representative of three independent experiments

previously demonstrated that vanadium compounds cause a reduction of tumor growth in both in vivo and in vitro systems [25, 29–31].

As part of a research project devoted to the investigation of vanadium complexes with potential pharmacological applications, we have tested the antitumoral effects of a complex of oxidovanadium(IV) and the flavonoid silibinin against osteosarcoma cells. Osteosarcoma is an aggressive malignant neoplasm arising from primitive transformed cells of mesenchymal origin that exhibit osteoblastic differentiation and produce malignant osteoid. It is the commonest histological form of primary bone cancer [64]. For this reason, we chose the MG-63 cell line derived from a human osteosarcoma because according to the literature it is a good model and one of the most used cell lines for bone cancer research [32].

In this work, we have investigated the cytotoxic and genotoxic effects of VOsil and we have also elucidated the putative mechanism of action underlying its effects.

Our results demonstrated the beneficial effect of complexation on the antitumoral action as shown in Fig. 2. VOsil caused the main deleterious action in the tumor cells in comparison with the oxidovanadium(IV) species and the free flavonoid silibinin. These results were similar to those obtained with another oxidovanadium(IV) complex with the flavonoid chrysin, for which the beneficial effects of metal coordination were also observed [18]. The antitumoral effects of VOsil were compared with those of the reference antitumor drug cisplatin, and our results showed quite good correlation between these two compounds, indicating that VOsil may be placed category of non-platinum antitumor drugs. Moreover, we have also investigated the effects of VOsil under more natural conditions, such as the presence of serum components. In fact, the complex could interact with different factors of the serum and this interaction could modify its antiproliferative action on MG-63 osteosarcoma cells. The cell viability experiments in the presence of the 10 % FBS and different concentrations of the VOsil showed no statistical differences with the effects of VOsil in the absence of serum. Similar results were obtained when the toxicity of VOsil was evaluated in the presence of FBS. As a whole, these results suggest that the interactions of the serum components with VOsil would be negligible in relation to its antitumoral activity.

On the other hand, the deleterious effect of VOsil was previously tested by our group on two osteoblast-like cell lines in culture: UMR106 derived from a rat osteosarcoma and a nontransformed osteoblast cell line, MC3T3-E1, derived from mouse calvaria [16]. Comparison of the antiproliferative effects of VOsil on the three osteoblast cell lines shows the potency increases in the order MC3T3-E1 < MG-63 < UMR106, with half-maximal inhibitory concentrations of 92, 74, and 51 μM, respectively. As a whole, these results indicate that VOsil had greater antiproliferative actions in the two tumor cell lines than in the nontransformed osteoblasts. Besides, no deleterious actions were detected in normal PMBCs at 25 and 50 μM and only a minimum effect was determined at 100 μM VOsil. Altogether, these results indicate that VOsil is an interesting candidate for potential antitumor uses. Similar results for other oxidovanadium(IV) complexes have been previously reported by Strianese et al. [65] in several cell lines.

Moreover, our results show that the cytotoxic effects of VOsil on MG-63 cells may be due to different causes, such as the functional disruption of several organelles such as the lysosomes and the mitochondria. Our findings demonstrate that the cytotoxic actions of VOsil affected the normal activity of the lysosomes and the mitochondria, contributing in this way to the deleterious effect of VOsil on the tumor cell line MG-63. Moreover, a probable toxic interaction between oxidative stress and disruption of lysosomal and mitochondrial metabolism can therefore be suggested.

Moreover, vanadium compounds may also exert antiproliferative effects via interactions with DNA. VOsil induced single-strand and double-strand DNA breaks in MG-63 cells, leading to a positive result in the comet assay and induction of micronuclei, which were significantly detected at lower concentrations of VOsil. DNA damage was also reported in human blood leukocytes exposed to vanadium oxides in vitro. It was observed that the genotoxic effect of vanadium can be produced by any of its three oxidation states. However, vanadium(IV) induces double-strand breaks, and it is believed that these lesions are linked to the formation of structural chromosomal aberrations [66]. Recently, we reported the genotoxic action of a oxidovanadium(IV) complex with the flavonoid chrysin $[VO(chrysin)_2EtOH]_2$ (Vochrys) in osteosarcoma cells [18]. For that complex, the genotoxic effect detected by the comet and micronucleus assays started at lower concentrations than for VOsil and showed a dose response correlation from 2.5 to 5 μM, with a less pronounced effect in the comet assay from 10 to 25 μM, probably related to overt cytotoxicity exerted by VOchrys on the MG-63 cell line. Moreover, we have previously described the genotoxic effect of another complex of the oxidovanadium(IV) cation with oxodiacetate from 10 μM in Caco-2 human colon adenocarcinoma cells. This action agreed with the effect on plasmidic DNA causing single-strand and double-strand cleavage [67]. Overall, we can conclude that the genotoxic effects exerted by oxidovanadium(IV)) complexes depend not only on the ligand but also on the cell line tested. On the other hand, we have previously reported the genotoxicity of hydroxylamido/amino acid complexes of oxidovanadium(IV) in osteoblast-like cells, showing a

cell-line-dependent effect [48]. Moreover, in vivo experiments showed the genotoxicity of tetravalent vanadium. Vanadyl sulfate in male CD1 mice produced an increase in the incidence of micronucleated blood reticulocytes and bone marrow polychromatic erythrocytes, in addition to DNA lesions detectable by the comet assay [68].

In an attempt to elucidate the mechanism of action involved in the effects of VOsil, we studied the oxidative stress (by means of ROS production) and GSH levels as well as the GSH/GSSG redox couple. In addition, an exhaustive study of apoptosis and cell cycle arrest was also performed. Our results showed that VOsil increased ROS production in a dose-dependent manner. The increase in ROS levels has been associated with cell death or membrane injury. It has been reported that high levels of ROS can induce apoptosis by triggering either the endoplasmic-reticulum-stress-mediated apoptotic pathway or the mitochondrial-mediated apoptotic pathway, or both. The elevation of cytosolic Ca^{2+} levels, due to endoplasmic-reticulum stress, may induce the mitochondrial permeability transition pore opening, cytochrome *c* release, and caspase cascade activation, and lead to apoptosis [69, 70]. Besides, it is generally known that the GSH-related thiols participate in many important biological reactions, including the protection of cell membranes against oxidative damage. Vanadium toxicity has been previously associated with its capacity to induce the formation of ROS, probably by interacting with mitochondrial redox centers [71]. Overall, it can be assumed that the free radicals decrease the concentration of important cellular compounds and impair the antioxidant system, making cells more vulnerable to oxidative damage. Similar results have been previously reported for other oxidovanadium(IV) complexes in osteoblast-like cells in culture [18, 49]. Moreover, vanadate, a vanadium(V) species, caused a further decrease of GSH levels in diabetic rat liver [72]. Besides, the GSH levels are related to the neoplastic transformation and toxicity in mouse embryo cells [73].

Vanadium compounds may also exert antiproliferative effects via induction of apoptosis. Our findings showed that the percentages of apoptotic and apoptotic/necrotic cells increased with the concentration of VOsil and the exposure time. These results are in accordance with the viability assays, confirming that the deleterious action of VOsil is dependent on its concentration in the MG-63 cell line. Previous results also showed that other vanadium compounds caused an increase in the number of apoptotic cells as a function of their concentration. In fact, simple inorganic vanadium(IV) and vanadium(V) compounds such as that $VOSO_4$, $NaVO_3$, and vanadium pentoxide induced apoptosis in different cell types [74–76]. Besides, vanadium(IV) and vanadium(V) with organic ligands induced oxidative stress on mitochondria and thus caused an increase in different apoptotic mechanisms [18, 76, 77]. Recent articles have shown that in isolated rat liver hepatocytes as well as in an N27 dopaminergic neuronal cell model, vanadium induced cytotoxicity and an increase in the levels of caspase 3 [78, 79]. Moreover, orthovanadate induced caspase-dependent apoptosis in thyroid cancer cells [74]. Collectively, the antiproliferative concentrations of the drug induce typical features of apoptosis, including phosphatidylserine externalization, production of ROS, and activation of caspase 3.

Similar results have been reported in the literature for a few of vanadium compounds. In fact, the apoptogenic effect of NH_4VO_3 on the MCF7 human breast cancer cell line was investigated by Ray et al. [80]. The exposure of the cells to vanadium led to the induction of apoptosis in a dose-dependent manner. Vanadium treatment brought about prominent chromatin condensation, cell cycle arrest, and apoptosis in these tumor cells. Besides, vanadyl bisacetylacetonate blocked cell cycle progression permanently at G_1 phase in a dose- and time-dependent manner in HepG2 cells [81].

Overall, our results demonstrate that the arrest of the cell cycle is one of the main processes that mediate the antiproliferative effect of VOsil, as was clearly shown through the increase of the sub-G_1 peak in a time- and a concentration-dependent manner discussed in detail before.

Conclusions

New vanadium complexes with potential antitumoral effects currently require more intensive basic and applied research since this knowledge obtained from in vitro studies may allow vanadium compounds to enter the preclinical in vivo phase. On these bases, we have thoroughly investigated the putative mechanisms underlying the antiproliferative effects of a complex of the oxidovanadium(IV) cation with the flavonoid silibinin, VOsil, in a human osteosarcoma cell line (MG-63). This research is intended to contribute to the body of knowledge of the chemical and biochemical properties as well as the mechanisms of the cellular and molecular antitumoral effects of vanadium compounds.

The exhaustive characterization of the putative mechanisms of action of VOsil was performed in the frame of a general research project devoted to the development of vanadium compounds with potential therapeutic applications. In particular, we have tried to contribute to the establishment of vanadium compounds as a new class of non-platinum, effective antitumor agents.

A comprehensive study was conducted for the first time on the promising antitumoral properties of VOsil in a human osteosarcoma cell line. We have demonstrated that

the complexation of the flavonoid silibinin with oxidovanadium(IV) improved the antitumoral activity of the ligand.

VOsil caused cytotoxicity and genotoxicity in a concentration-dependent manner. It interacted with lysosomes and mitochondria as well as with cellular DNA. VOsil increased the ROS level and arrested the cell cycle at G_2/M phase. Besides, the complex induced early and late apoptotic events in a dose-dependent manner. As a whole, these results indicate that VOsil is an interesting candidate for potential antitumor uses, and provide new insight into the development of vanadium compounds as potential anticancer agents.

Acknowledgments This work was partly supported by UNLP (11X/554), CONICET (PIP 1125), and ANPCyT (PICT 2008-2218 and PICT-2010-0981) from Argentina. A.L.D.V.and S.B.E. are members of the Carrera del Investigador, CONICET, Argentina. P.A.M.W. is member of the Carrera del Investigador, CIC, and PBA. I.E.L. has a fellowship from ANPCyT, Argentina, and a fellowship from AMSUD- PASTEUR, Institut Pasteur, Uruguay. L.G.N. has a postdoctoral fellowship from CONICET, Argentina. V.P. and M.B.F. are members of the Sistema Nacional de Investigadores of the Agencia Nacional de Investigación e Innovación in Uruguay. The authors would like to thank Inés Tiscornia for the management work with the cells and Miguel Reigosa for help with the PMBC assay. Moreover, the authors would like to thank M.C. Bernal for her careful revision of the manuscript.

References

1. Beecher GR (2003) J Nutr 133:3248S–3254S
2. Ferrer EG, Williams PAM (2011) Modification of flavonoid structure by oxovanadium(IV) complexation. Biological effects. In: Yamane K, Kato Y (eds) Handbook on flavonoids: dietary sources, properties and health benefits. Nova, Hauppauge, pp 145–190
3. Kima JD, Liub L, Guob W, Meydani M (2006) J Nutr Biochem 17:165–176
4. Valko M, Leibfritz D, Moncol J, Cronin MTD, Mazur M, Telser J (2007) Int J Biochem Cell Biol 39:44–84
5. Gazák R, Walterova D, Kren V (2007) Curr Med Chem 14:315–338
6. Svagera Z, Skottová N, Vána P, Vecera R, Urbánek K, Belejová M, Kosina P, Simánek V (2003) Phytother Res 17:524–530
7. Varga Z, Czompa A, Kakuk G, Antus A (2001) Phytother Res 15:608–612
8. Ge Y, Zhang Y, Chen Y, Li Q, Chen J, Dong Y, Shi W (2011) Int J Mol Sci 12:4861–4871
9. Agarwal C, Wadhwa R, Deep G, Biedermann D, Gažák R, Křen V, Agarwal R (2013) PLoS One 8:e60074. doi:10.1371/journal.pone.0060074
10. Singh RP, Agarwal R (2004) Curr Cancer Drug Targets 4:1–11
11. Mokhtari MJ, Motamed N, Shokrgozar MA (2008) Cell Biol Int 32:888–892
12. Bhatia N, Zhao J, Wolf DM, Agarwala R (1999) Cancer Lett 147:77–84
13. Hogan FS, Krishnegowda NK, Mikhailova M, Kahlenberg MS (2007) J Surg Res 143:58–65
14. Kauntz H, Bousserouel S, Gosse F, Marescaux J, Raul F (2012) Int J Oncol 41:849–854
15. Kauntz H, Bousserouel S, Gosse F, Raul F (2013) Oncol Lett 5:1273–1277
16. Naso LG, Ferrer EG, Butenko N, Cavaco I, Lezama L, Rojo T, Etcheverry SB, William PAM (2011) J Biol Inorg Chem 16:653–668
17. Kuntić V, Filipović I, Vujić Z (2011) Molecules 16:1378–1388
18. Leon IE, Di Virgilio AL, Porro V, Muglia CI, Naso LG, Williams PAM, Bollati-Fogolin M, Etcheverry SB (2013) Dalton Trans 42:11868–11880
19. Nielsen FH (1995) In: Sigel H, Sigel A (eds) Metal ions in biological systems, vanadium and its role in life. Dekker, New York, pp 543–574
20. Slebodnicj C, Hamstra BJ, Pecoraro VL (1997) Struct Bonding 89:51–107
21. Srivastava K, Mehdi MZ (2004) Diabetic Med 22:2–13
22. Cortizo AM, Etcheverry SB (1995) Mol Cell Biochem 145:97–102
23. Etcheverry SB, Barrio DA (2007) In: Kustin K, Costa Pesoa J, Crans DC (eds) Vanadium: the versatile metal. ACS symposium series, vol 974. American Chemical Society, Washington, pp 204–216
24. Djordjevic C, Wampler GL (1985) J Inorg Biochem 25:51–55
25. Evangelou AM (2002) Crit Rev Oncol Hematol 42:249–265
26. Kris-Etherton PM, Hecker KD, Bonanome A, Coval SM, Binkoski AE, Hilpert KF, Griel AE, Etherton TD (2002) Am J Med 113:71–88
27. Bhuiyan MS, Fukunaga K (2009) J Pharmacol Sci 110:1–13
28. Shioda N, Han F, Fukunaga K (2009) Int Rev Neurobiol 85:375–387
29. Etcheverry SB, Williams PAM (2009) New developments in medicinal chemistry. In: Ortega MP, Gil IC (eds) Medicinal chemistry of copper and vanadium bioactive compounds. Nova, Hauppauge, pp 105–129
30. Barrio DA, Etcheverry SB (2010) Curr Med Chem 17:3632–3642
31. Djordjevic C (1995) In: Sigel H, Sigel A (eds) Metal ions in biological systems, vanadium and its role in life. Dekker, New York, pp 595–616
32. Mohseny AB, Pancras CW, Hogendoorn CW, Cleton-Jansen AM (2012) Sarcoma. doi:10.1155/2012/417271
33. Nicoletti I, Migliorati G, Pagliacci MC, Grignani F, Riccardi C (1991) J Immunol Methods 139:271–280
34. Okajima T, Nakamura H, Zhang Y, Ling N, Tanabe T, Yasuda T, Rosenfeld RG (1992) Endocrinology 130:2201–2212
35. Borenfreund E, Puerner JA (1984) J Tissue Cult Methods 9:7–9
36. Mosmann T T (1983) J Immunol Methods 65:55–63
37. Fenech M (2000) Mutat Res 455:81–95
38. Fenech M (1993) Mutat Res 1:35–44
39. Singh NP, McCoy MT, Tice RR, Schneider EL (1988) Exp Cell Res 1988(175):184–191
40. Cortizo AM, Bruzzone L, Molinuevo MS, Etcheverry SB (2000) Toxicology 147:89–99
41. Hissin PJ, Hilf R (1976) Anal Biochem 74:214–226
42. Bradford M (1976) Anal Biochem 72:248–254
43. Hurley AA (2001) Curr Protoc Cytom 7.2.1–7.2.5
44. Pozarowski P, Grabarek J, Darzynkiewicz Z (2003) Curr Protoc Cytom 25:7.19.1–7.19.33
45. Stopper H, Muller SO (1997) Toxicol In Vitro 11:661–667
46. Collins AR, Dobson VL, Dusinka M, Kennedy G, Stetina R (1997) Mut Res 375:183–193
47. Liao W, Nutt MA, Zhu MG (2009) Methods 48:46–53
48. Leon IE, Di Virgilio AL, Barrio DA, Arrambide G, Gambino D, Etcheverry SB (2012) Metallomics 4:1287–1296
49. Rivadeneira J, Di Virgilio AL, Barrio DA, Muglia CI, Bruzzone L, Etcheverry SB (2010) Med Chem 6:9–23

50. Ye J, Ding M, Leonard SS, Robinson VA, Millecchia L, Zhang X, Castranova V, Vallyathan V, Shi X (1999) Mol Cell Biochem 202:9–17
51. Zhang Z, Huang C, Li J, Leonard SS, Lanciotti R, Butterworth L, Shi X (2001) Arch Biochem Biophys 392:311–332
52. Capella MAM, Capella LS, Valente RC, Gefe′ M, Lopes AG (2007) Cell Biol Toxicol 23:413–420
53. Jones DP, Carlson JL, Mody VC, Cai JY, Lynn MJ, Sternberg P (2000) Free Radic Biol Med 28:625–635
54. Hwang C, Sinskey AJ, Lodish HF (1992) Science 57:1496–1502
55. Nicholson DW, Ali A, Thornberry NA, Vaillancourt JP, Ding CK, Gallant M, Gareau Y, Griffin PR, Labelle M, Lazebnik YA (1995) Nature 376:37–43
56. Sakahira H, Enari M, Nagata S (1998) Nature 391:96–99
57. Kamada S, Kusano H, Fujita H, Ohtsu M, Koya RC, Kuzumaki N, Tsujimoto Y (1998) Proc Natl Acad Sci USA 95:8532–8537
58. Porter AG, Janicke RU (1999) Cell Death Differ 6:99–104
59. Sherr CJ (2000) Cancer Res 60:3695–3698
60. Kerr JFR, Wyllie AH, Curie AR (1972) Br J Cancer 26:239–257
61. Arends MJ, Morris RG, Wyllie AH (1990) Am J Pathol 136:593–608
62. Nagata S (2000) Exp Cell Res 256:12–18
63. Umansky SR, Korol BA, Nelipovich PA (1981) Biochim Biophys Acta 655:9–17
64. Ottaviani G, Jaffe N (2009) The epidemiology of osteosarcoma. In: Jaffe N et al (eds) Pediatric and adolescent osteosarcoma. Springer, New York
65. Strianese M, Basile A, Mazzone A, Morello S, Turco MC, Pellecchia C (2013) J Cell Physiol 228:2202–2209
66. Rodriguez-Mercado JJ, Mateos-Nava RA, Altamirano-Lozano MA (2011) Toxicol In Vitro 25:1996–2002
67. Di Virgilio AL, Rivadeneira J, Muglia CI, Reigosa MA, Butenko N, Cavaco I, Etcheverry SB (2011) Biometals 24:1153–1168
68. Villani P, Cordelli PE, Leopardo P, Siniscalchi E, Veschetti E, Fresegna AM, Crebelli R (2007) Toxicol Lett 170:11–18
69. Wang CC, Chiang YM, Sung SC, Hsu YL, Chang JK, Kuo PL (2008) Cancer Lett 259:82–98
70. Baumgartner HK, Gerasimenko JV, Thorne C, Ashurst LH, Barrow SL, Chvanov MA, Gillies S, Criddle DN, Tepikin AV, Petersen OH, Sutton R, Watson AJM, Gerasimenko OV (2007) Am J Physiol Gastrointest Liver Physiol 293:296–307
71. Valko M, Morris H, Cronin MT (2005) Curr Med Chem 12:1161–1208
72. Saxena AK, Srivastava P, Kale RK, Baquer NZ (1993) Biochem Pharmacol 45:539–542
73. Sabbioni E, Pozzi G, Devos S, Pintar A, Casella L, Fischbach M (1993) Carcinogenesis 14:2565–2568
74. Gonçalves AP, Videira A, Soares P, Maximo V (2011) Life Sci 12:11–12
75. Montiel-Davalos A, Gonzalez-Villava A, Rodriguez-Lara V, Montano LF, Fortoul TI, Lopez-Marure R (2012) J Appl Toxicol 32:26–33
76. Zhao Y, Ye L, Liu H, Xia Q, Zhang Y, Yang X, Wang K (2010) J Inorg Biochem 104:371–378
77. Rivadeneira J, Barrio DA, Arrambide G, Gambino D, Bruzzone L, Etcheverry SB (2009) J Inorg Biochem 103:633–642
78. Hosseini MJ, Seyedrazi N, Shahraki J, Pourahmad J (2012) Adv Biosci Biotechnol 3:1096–1103
79. Afeseh Ngwa H, Kanthasamy A, Anantharam V, Song C, Witte T, Houk R, Kanthasamy AG (2009) Toxicol Appl Pharmacol 240:273–285
80. Ray RS, Rana B, Swami B, Venu V, Chatterjee M (2006) Chem Biol Interact 163:239–247
81. Fu Y, Wang Q, Yang XG, Yang XD, Wang K (2008) J Biol Inorg Chem 13:1001–1009